AIP | Review of Scientific Instruments

Simple flow microphotometer for rapid cell population analysis

W. G. Eisert, R. Ostertag, and E.G. Niemann

Citation: Review of Scientific Instruments **46**, 1021 (1975); doi: 10.1063/1.1134399
View online: http://dx.doi.org/10.1063/1.1134399
View Table of Contents: http://scitation.aip.org/content/aip/journal/rsi/46/8?ver=pdfcov
Published by the AIP Publishing

Articles you may be interested in

Power flow analysis of simple structures
J. Acoust. Soc. Am. **84**, 1557 (1988); 10.1121/1.397229

Design of stoppedflow NMR rapidmixing cells
Rev. Sci. Instrum. **46**, 1201 (1975); 10.1063/1.1134445

A Simple Method to Rapidly Advance Microelectrodes into Biological Cells
Rev. Sci. Instrum. **43**, 941 (1972); 10.1063/1.1685815

A Simple Automatic Recording Microphotometer
Rev. Sci. Instrum. **21**, 938 (1950); 10.1063/1.1745472

Accurate, Simple Recording Microphotometer
Rev. Sci. Instrum. **20**, 321 (1949); 10.1063/1.1741518

This article is copyrighted as indicated in the article. Reuse of AIP content is subject to the terms at: http://scitationnew.aip.org/termsconditions. Downloaded to IP: 146.107.3.4 On: Fri, 28 Nov 2014 09:44:15

Simple flow microphotometer for rapid cell population analysis

W. G. Eisert, R. Ostertag*, and E.-G. Niemann

Gesellschaft für Strahlen- und Umweltforschung mbH., Institut für Strahlenbotanik, 3 Hannover, Herrenhäuserstr. 2, West Germany

(Received 11 March 1975; in final form 21 April 1975)

A simple particle analyzer has been developed using a modified high speed flow-through technique and absorption measurements of a continuous He–Ne laser beam. From pulse-shape analysis and the integration of absorption pulses, size distributions of stained or unstained cells can be derived. The range of 5–300 μ is covered without changing the flow system and a rate up to 200 000/sec can be achieved. Typical applications in cell analyses are shown.

I. INTRODUCTION

The problem of cell sorting and counting has been treated in a number of papers recently. Described for several years,[1–11] these and partly commercially available systems use light scattering and fluorescence only or in combination to differentiate cell classes. In some cases these optical parameters have been combined with the Coulter principle. Most of these high speed cell counters use a hydrodynamic focusing flow chamber, which allows a cell by cell examination of the sample and is known in literature.

The hydrodynamic focusing system places the optical axis perpendicular to the direction of flow. It has been compared with mechanical focusing by a narrow capillary tube or bore and a sample flow in the direction of the optical axis.[12,13] For the examination of particles and cells with a size distribution from 5 to 300 μ without changing the flow chamber, only the hydrodynamic focusing seems to be useful.

In the following a simpler and less expensive system is described obtaining cell data from the measurement of the transmitted light of a He–Ne laser. The construction of the flow chamber has been modified for this purpose. Typical measurements on *Tetrahymena pyriformis* L. and on blood particles are discussed.

II. PRINCIPLE OF OPERATION

It has been shown that in a laminar flow of a hydrodynamic focused system dispersed cells of nonspherical forms are oriented in the streaming axis towards the direction of flow. Mammalian erythrocytes are deformed into ellipsoid-like bodies. The ratios of the ellipsoid axes vary from 4:1:1 to 2:1:1 dependent on the nature of the suspension medium.[14] If a single file cell stream is oriented perpendicular to the optical axis and meets the focus of a laser beam [Fig. 1(a)], the absorbance of a slice of the passing cell can be measured [Fig. 1(b)].

The extinction of light following Lambert's law is not the only cause of losses from the incident light beam. Cell constituents scatter light out of the collection cone. These so-called nonspecific losses lead to a detectable "absorption" signal even when the cell is not stained.

When certain conditions are obeyed, the half-width of the detected absorption pulse is proportional to the length of the cell or particle:

(1) The maximum radius of the light beam that the cells pass through must be at least several times smaller than the minimum size of the cells.

(2) The velocity of the particle stream must be kept constant during the period of measurement.

(3) Displacement of the cells in the plane perpendicular to the direction of flow must not exceed one-half of the cell diameter.

The measurement of the cell length can be combined with the measurement of the absorption of the cell scan to obtain the integral of the absorption pulse. Cell populations of the same size distribution but of different staining can be discriminated in this way. The values of pulse length and pulse integral are converted into short "needle" pulses of proportional heights, which can be discriminated on a multichannel pulse height analyzer.

III. THE FLOW-THROUGH SYSTEM

A schematic of the hydrodynamic focusing flow system is shown in Fig. 2. The flow-through is achieved by a

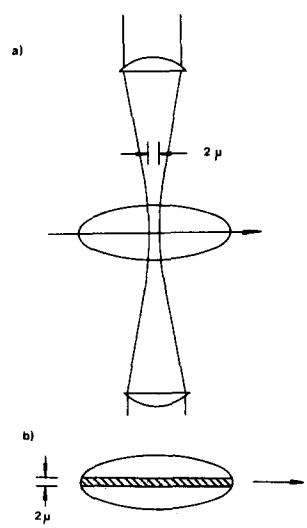

FIG. 1. Principle of measurement. (a) The single file cell stream passes the beam waist of the laser beam. The cell stream axis is adjusted at focus. (b) The absorption of a slice of the passing particle is measured under constant flow conditions. Particle data are derived from pulse-shape analysis.

 Copyright © 1975 by the American Institute of Physics

This article is copyrighted as indicated in the article. Reuse of AIP content is subject to the terms at: http://scitationnew.aip.org/termsconditions. Downloaded to IP: 146.107.3.4 On: Fri, 28 Nov 2014 09:44:15

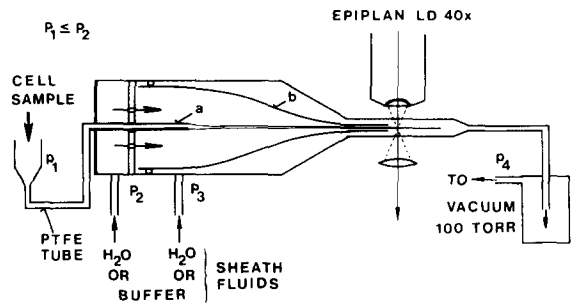

FIG. 2. Flow-through system. The sample suspension is inserted in the system through a Teflon tube (a) in the region of laminar flow of sheath fluid (1). The sheath tube (b) forms the hydrodynamic focusing unit and ends in front of the optical axis. Sheath fluid (2) allows index matching for plane viewing windows. A constant negative pressure (100 Torr) keeps flow conditions stable.

constant vacuum p_4, with a typical value between 80 and 100 Torr depending on the experiment.

The probe is inserted through a 0.4 mm i.d. Teflon (PTFE) capillary tube (a). The outlet of the Teflon tube is in the region of laminar flow of the sheath fluid (1). If the pressure of the sheath fluid (1) is slightly higher than the pressure of the probe, a narrowing of the probe beam at the outlet of the sample tube results (typical $\Delta p \sim 10$ mm H_2O). Hydrodynamic focusing is achieved by a special formed glass tube (b) which is surrounded by a second sheath fluid (2). This enables good optical index matching between the probe beam and the optical system. The inner diameter at the end of the focusing glass tube is typically 0.3 mm, resulting in a probe beam diameter of 4 μ. Therefore, the minimum diameter for correct focus upon cells is the same. The limitation for the maximum particle diameter is given by the inner diameter of the glass tube. By changing the glass tube (b) other size ranges can be covered.

In contrast to earlier designs,[13,15] our measurement area was behind the outlet of the glass tube. The jet, consisting of probe and sheath fluid (1), is stable over a distance of several millimeters. Therefore, proper index matching is achieved, and the dispersing effects of the two concave cylindrical lenses formed by the capillary walls are avoided. The velocity of the probe beam in the measurement area is typically 2 m·sec^{-1}.

IV. OPTICAL ARRANGEMENT

A simple microscope was slightly modified for the optical arrangement (Fig. 3). Two beam splitters were installed to separate the He–Ne laser beam from the optical control for correct beam adjustment. To protect the operator's eyes several highly reflecting laser mirrors were installed in the eyepiece resulting in narrow band blocking at the laser frequency (6328 Å) down to 10^{-6}. A long distance objective with a magnification of 40 (Epiplan 40, Zeiss) focused the laser beam. The resulting minimum spot diameter could be measured as <1 μ. The laser focus was adjusted in the object plane by a correction lens (CL) to allow optical control of the probe beam.

To avoid errors due to scattered light only a cone of 1° or 2° solid angle was detected by the photoreceiver.

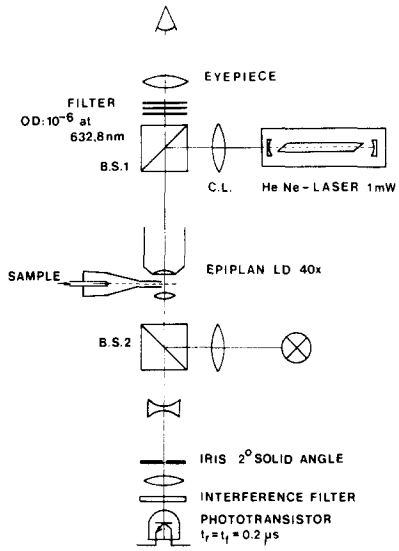

FIG. 3. Optical arrangement. Two beamsplitters (BS 1, BS 2) separate the laser detecting beam from the viewing pathway. A correction lens (CL) adjusts the laser focus in the vision plane of the microscope. Only light of a solid angle smaller than 2° is able to pass the combination biconcave lens–iris. Three laser mirrors are installed as filters in the eyepiece to protect operator's eyes.

For this purpose two biconcave lenses ($f = -25$ mm) were installed in the microscope condenser, and an iris was placed in front of the receiver unit. A narrow band interference transmission filter (IF) for the laser wavelength allowed operation in illuminated rooms. A phototransistor (BPY 62, Siemens) in combination with a transistor compensation unit[16] served as photoreceiver unit, with a rise and fall time of 0.2 μsec. By monitoring the output of our He–Ne laser (CW Radiation Inc., S-100; 1 mW) and using feedback regulation of the power supply, a long time stability of $<1\%$ was achieved.

V. SIGNAL PROCESSING

A schematic of the signal processing is shown in Fig. 4 along with a photograph of a typical absorption pulse. Three simple analog computers[17] served as interfaces to a multichannel analyzer, which displayed the distribution of one chosen parameter. Each analog computer delivered a pulse of a constant shape at its output, which was detected

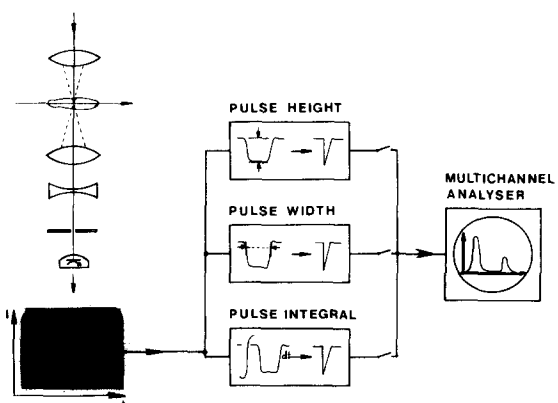

FIG. 4. Signal processing. The detected absorption pulse of a passing cell is shown at the left. "Needle" pulses of constant shapes but of pulse heights proportional to the input pulse height, pulse width or pulse integral are formed in the electronic setup. The distribution of one of these parameters can be displayed by a multichannel pulse-height analyzer.

This article is copyrighted as indicated in the article. Reuse of AIP content is subject to the terms at: http://scitationnew.aip.org/termsconditions. Downloaded to IP: 146.107.3.4 On: Fri, 28 Nov 2014 09:44:15

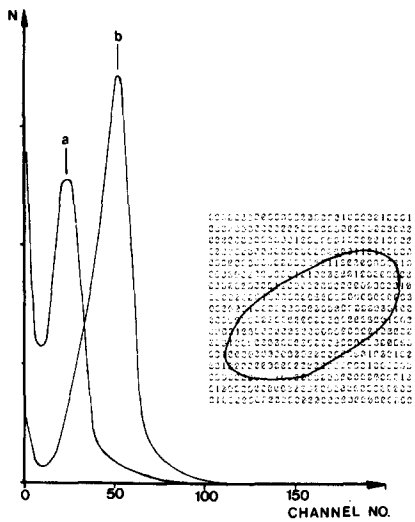

FIG. 5. Size distributions of unstained *Tetrahymena pyriformis* L. derived from absorption pulse width. Two populations with average cell lengths of 40 μ (size 1) and 80 μ (size 5), respectively. Right—Absorption scan (Zeiss Cytoscan) of an unstained ciliate at the laser wavelength (6328 Å). Pulse width: a—size 1 (40 μ); b—size 5 (80 μ).

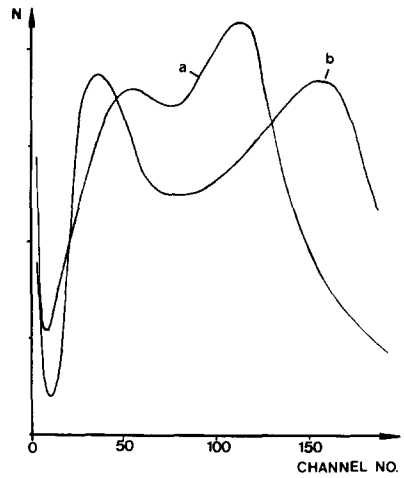

FIG. 7. Size distributions of two mixed populations (*Tetrahymena pyriformis* L., stained) derived from absorption pulse width (a) and from absorption pulse integral (b). a—Pulse width; b—pulse integral.

by the multichannel analyzer. The pulse height was made proportional either to the pulse width or to the pulse integral. Also, a conversion had to be applied for the pulse height of pulses with long half-widths and different pulse shapes, due to the input requirements of the multichannel analyzer.

The flow system and the analog computers allowed a pulse rate of more than 200 000/sec in a single file, but this rate was limited by the conversion rate and memory cycling of the multichannel analyzer. In our case we could go up to 50 000/sec. If one were interested only in the upper part of a size distribution, the flow system could be run at a higher velocity and the bulk of smaller pulses then discriminated out rather than entering the multichannel analyzer.

VI. APPLICATIONS

The system so far has been applied to measurements with *Tetrahymena pyriformis* L., red blood cells, and blood aggregates. The size of the ciliate *Tetrahymena* is correlated with the mass of protein in the cells. Therefore, a correlation to protein content can be derived from the length of the ellipsoidal bodies of the animals. We compared three populations. Unstained cells of size 1 and size 5 were compared in one experiment (Fig. 5), and the stained cells of size 1 and size 4 were compared in another experiment (Fig. 6). The size distributions of the two populations in both cases are in good agreement with the conventionally measured and counted values. The right-hand sides of the figures show the distributions of the absorption values over the cell area measured with a microspectrophotometer (Zeiss Cytoscan) at the laser wavelength. The numbers represent the absorption values, i.e., 0=0%–9% absorption; 1=10%–19% absorption; . . . . Figure 5 demonstrates that cell size distribution can be obtained with unstained cells.

A comparison of the information from the particle length and the combined information from the integral of the absorption pulses is shown in Fig. 7. As mentioned above, higher protein content leads to higher absorption values of stained cells. A mixture of two cell populations which hardly can be separated into two classes by measuring cell lengths can easily be separated by looking at the distribution of the integral values of the absorption pulses.

The system is presently applied in routine controls of the size distributions of blood particles in native and stored blood.[18] For this application it is not advantageous to do any staining because this would affect the agglutination of

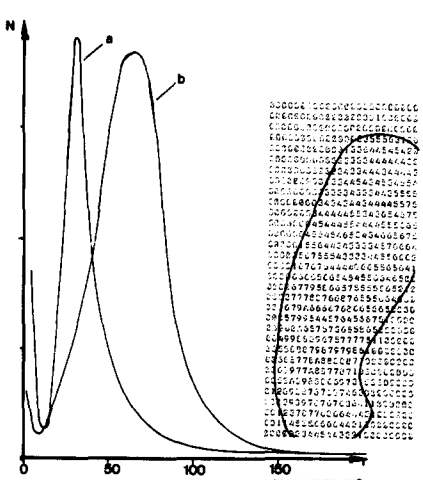

FIG. 6. Size distributions of stained (naphthol blue-black) *Tetrahymena pyriformis* L. derived from absorption pulse width. Two populations with average cell lengths of 40 μ (size 1) and 70 μ (size 4), respectively. Right—absorption scan at the laser wavelength (6328 Å). Pulse width: a—size 1 (40 μ); b—size 4 (70 μ).

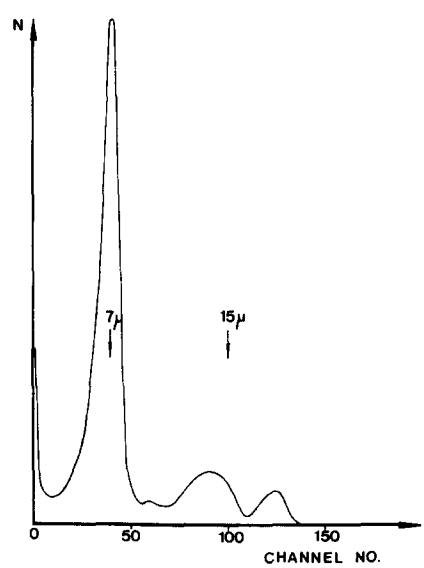

FIG. 8. Size distribution of fresh erythrocytes (unstained) derived from absorption pulse widths.

This article is copyrighted as indicated in the article. Reuse of AIP content is subject to the terms at: http://scitationnew.aip.org/termsconditions. Downloaded to IP: 146.107.3.4 On: Fri, 28 Nov 2014 09:44:15

blood cells and influence the size distribution. A typical result for blood particles is shown in Fig. 8.

VII. DISCUSSION

The coefficient of variation in the *Tetrahymena* experiments was about 5%, as estimated from comparison of the machine data with the hand-measured distributions. As can be seen from the blood cell data, particles down to 5 μ can be resolved. Variations are caused only by the relative instability of the probe beam in the hydrodynamic focusing system. Electronic simulation of the absorption pulses by a pulse generator did not show any variation in the electronic device. The size distribution of the erythrocytes is in good agreement with Coulter counter measurements.

Relative calibration of particle diameter can be achieved by defining the erythrocyte peak as 7 μ. By simulating the electronic signal caused by an erythrocyte in the optical detector and subsequently stretching the half-width of the simulating pulse in terms of one erythrocyte half-width, one can calibrate for particle diameter.

The 1 mW laser power seems to be the minimum permissible for light detection by inexpensive phototransistors. Greater power should be used when measuring rather weakly absorbing particles (1%–2% absorption) to avoid noise problems. For simultaneous fluorescence detection a He–Cd or Ar laser could be used instead of the He–Ne laser and an additional photomultiplier used as fluorescence detector.

*Medizinische Hochschule Hannover, Dept. Innere Medizin, Abt. Klinische Immunologie und Transfusionsmedizin, 3 Hannover, Karl-Wiechert-Allee 9, Federal Republic of Germany.

[1]M. A. Van Dilla, T. T. Trujillo, P. F. Mullaney, and J. R. Coulter, Science **163**, 1213 (1969).
[2]H. R. Hulett, W. A. Bonner, J. Barrett, and L. A. Herzenberg, Science **166**, 747 (1969).
[3]W. A. Bonner, H. R. Hulett, R. G. Sweet, and L. A. Herzenberg, Rev. Sci. Instrum. **43**, 407 (1972).
[4]E. Sprenger, W. Sandritter, N. Bohm, M. Schaden, M. Hilgarth, and D. Wagner, Beitr. Pathol. Anat. Allg. Pathol. **143**, 323 (1971).
[5]J. A. Steinkamp and D. L. Carlson, Biomed. Sci. Instrum. **7**, 10 (1970).
[6]W. Dittrich and W. Göhde, Z. Naturforsch. B **24**, 360 (1969).
[7]J. A. Steinkamp, M. J. Fulwyler, J. R. Coulter, R. D. Hiebert, J. L. Horney, and P. F. Mullaney, Rev. Sci. Instrum. **44**, 1301 (1974).
[8]H. A. Crissman and R. A. Tobey, Science **184**, 1297 (1974).
[9]J. A. Steinkamp, A Romero, P. K. Horan, and H. A. Crissman, Exp. Cell. Res. **84**, 15 (1974).
[10]D. M. Holm and L. S. Cram, Exp. Cell. Res. **80**, 105 (1973).
[11]W. Göhde and W. Dittrich, Z. Anal. Chem. **252**, 328 (1970).
[12]P. J. Crosland-Taylor, Nature **4340**, 37 (1953).
[13]G. v. Sengbusch and B. Hugemann, Exp. Cell Res. **86**, 53 (1974).
[14]V. Kachel, Microscopia Acta **75**, 419 (1974).
[15]L. A. Kamemtsky, Advances in Biological and Medical Physics (Academic, New York, 1973), Vol. 14, p. 93.
[16]Siemens, *Schaltbeispiele* (Siemens Press, 8 München 80, 1974/75), p. 80.
[17]W. G. Eisert and E.-G. Niemann (private communication).
[18]R. Ostertag, W. G. Eisert, E.-G. Niemann, and H. Deicher (private communication).

This article is copyrighted as indicated in the article. Reuse of AIP content is subject to the terms at: http://scitationnew.aip.org/termsconditions. Downloaded to IP: 146.107.3.4 On: Fri, 28 Nov 2014 09:44:15